

A three-dimensional rotating rigid units network exhibiting negative Poisson's ratios

Daphne Attard^{*1} and Joseph N. Grima^{1,2}

¹ Faculty of Science, Department of Chemistry, University of Malta, Msida Malta, MSD 2080, Malta

² Faculty of Science, Metamaterials Unit, University of Malta, Msida Malta, MSD 2080, Malta

Received 29 June 2011, revised 25 April 2012, accepted 26 April 2012

Published online 25 May 2012

Keywords deformation, 3D models, negative Poisson's ratio, rotating rigid units

* Corresponding author: e-mail auxetic@um.edu.mt, Phone: +356 2340 2274, Fax: +356 2540 1091, Web: www.auxetic.info

Materials exhibiting auxetic behaviour get fatter when stretched (i.e. possess a negative Poisson's ratio). This property has been closely related to particular geometrical features of a system and how it deforms. One of the mechanisms which is known to have a potential to generate such behaviour is that of rotating rigid units. Several models based on this concept have been developed, including two-dimensional as well as three-

dimensional (3D) models. In this work, we propose a new 3D structure constructed from rigid cuboids which also deform through relative rotation of the units. In particular, analytical models for the mechanical properties, namely the Poisson's ratio and the Young's moduli, are derived and it is shown that for loading on-axis, these systems have the potential to exhibit negative values for all the six on-axis Poisson's ratios.

© 2012 WILEY-VCH Verlag GmbH & Co. KGaA, Weinheim

1 Introduction When a material is uniaxially stretched, the deformation along the stretching direction is normally accompanied by changes in its lateral dimensions. These changes are conveniently measured through the Poisson's ratio, a property which quantifies the changes in the aspect ratios of particular planes of a material when it is subjected to a uniaxial strain, ε_i , in that plane. More specifically, the Poisson's ratio ν_{ij} in the Ox_i – Ox_j plane for loading in the Ox_i direction is defined as:

$$\nu_{ij} = -\frac{\varepsilon_j}{\varepsilon_i} \quad (i, j = 1, 2, 3),$$

where ε_j is the strain in the direction perpendicular to that of loading. Everyday experience makes us intuitively assume that materials must become thinner when uniaxially stretched. In these cases the Poisson's ratio assumes positive values. But this is not always the case and in fact, it has long been known that it is possible for a material to have a negative Poisson's ratio. Such materials, more commonly referred to as auxetic [1], become fatter when stretched.

Apart from being an anomalous property, a negative Poisson's ratio is known to impart on materials several enhanced characteristics such as increased resilience and indentation resistance [2–6], pore size tunability [7–9] and better energy absorption and acoustic properties [10–15].

These enhanced characteristics make a negative Poisson's ratio a highly desirable property in materials as they can be used in several practical applications ranging from smart filters to protective equipment.

In recent years various new auxetic materials or structures have been designed, discovered and/or manufactured, which materials range from macroscale honeycomb structures [16–18] to nanoscale auxetic crystalline materials such as silicates [19–27] and zeolites [28–31].

Research carried out in the past decades clearly suggests that the sign and magnitude of the Poisson's ratio may be explained by looking at how particular geometric features present in the nano- or microstructure of materials deform when the material is subjected to a uniaxial stress (the deformation mechanism). These observations triggered various studies that have attempted to propose, develop or improve mechanistic models based on particular geometries which can result in negative Poisson's ratios. These include models based on flexure and hinging of re-entrant honeycombs [2, 16, 17, 32–35], rotation of rigid and semi-rigid units [23, 25, 36–40], models based on hard spheres [41–43], hard disks [44, 45], polydisperse systems [46], chaotic systems [47] dilatary/sliding models [23, 30, 48–54] and models based on chiral geometries [18, 55, 56]. Of particular interest in this respect is the fact that the Poisson's ratio is a scale independent

property, such that the same geometry-deformation mechanism model may operate at the macroscale, microscale as well as at the nanoscale. This is clearly illustrated by rotating rigid units systems which have been applied to a wide range of materials including microstructured polymeric auxetic foams where the rigid units represent mm– μ m features in the foams [57, 58], and crystalline materials such as zeolites where the rigid units correspond to features at the atomic (nano) scale [28, 31, 40, 59].

Using these rotating rigid units models, it has been shown that auxetic behaviour may be achieved through two-dimensional (2D) models involving rotation of rigid units which may also be accompanied by additional modes of deformation. Such 2D models are very useful as they may explain the Poisson's ratios of real three-dimensional (3D) systems by looking at their 2D projection in some particular plane. Nevertheless, it is obvious that such models also have their limitations, such as their inability to exhibit or explain concurrent in-plane and out-of-plane auxeticity. Such properties require the use of more complex models which must necessarily be of a 3D nature.

The concept of using 3D structures to predict or explain auxetic behaviour is not new. In fact, some of the pioneering work in the field of auxetics was based on 3D structures. These include the re-entrant structures proposed by Evans et al. [32], the tetrakaidecahedron with re-entrant features proposed by Choi and Lakes [34], and the 3D rotating and/or dilating tetrahedral model proposed and derived by Alderson et al. [23–25, 37] The latter works are of particular significance not only because they have shown that such models can explain extremely well the mechanical properties of real crystalline auxetic materials such as α -cristobalite but also because they represent the first attempt to achieve auxetic behaviour in terms of rotating rigid or semi-rigid units.

The work presented here aims to further expand on this earlier work by considering 3D models which are constructed from cuboidal shaped units which are connected to each other in such a way so as to permit relative rotation of the rigid cuboids. In particular, an attempt is made to derive the on-axis Poisson's ratios and Young's moduli of these systems, which may be considered to be the 3D equivalents of the 2D systems studied before. Furthermore, an attempt will be made to show how 2D models of projections can be used to predict the Poisson's ratio of such systems in particular planes, thus confirming the importance of both the 3D and much simpler 2D models to explain auxetic behaviour.

2 Analytical models In this section, a system constructed from cuboids connected at their edges which rotate with respect to each other is proposed. Expressions for its mechanical properties as a 3D structure are derived and it is shown that such a structure may exhibit auxetic behaviour in any of the three directions. A simplified version of this model, which considers a 2D projection of the system is also presented.

2.1 The three-dimensional model As illustrated in Fig. 1, the unit cell of the modelled 3D structure has three

planes of symmetry and can be described in terms of two hexagonal honeycomb cells connected perpendicular to each other with a face of a cuboidal unit sharing one of the faces of the honeycombs, as shown in Fig. 1a, so that the structure contains a total of ten cuboids. Since the hexagonal cells can be allowed to have different aspect ratios, cuboids having different sizes can be used, although the connectivity reduces the number of independent geometric parameters. In particular, in the case considered here, three different types of cuboids are used: two $a_1 \times b_1 \times c_1$,¹ four $a_2 \times b_2 \times c_2$ where $c_2 = c_1$ and four $a_3 \times b_3 \times c_3$ where $a_3 = a_1$ arranged as shown in Fig. 1b, so that a total of eight geometric parameters are required to fully describe the structure: $a_1, b_1, c_1, a_2, b_2, b_3, c_3$ and θ , which is defined as the angle between two $a_2 \times b_2 \times c_2$ cuboids. It is important to note that this structure is tessellatable and in fact can be used as the basic unit cell to construct larger structures such as the one shown in Fig. 1c. Note also that since in the presented model, the cuboids are assumed to remain rigid through the deformation, the geometric parameters a_i, b_i and c_i remain fixed, which means that the shape and size of any given system will be dependent on a single variable, θ . In fact, although in Fig. 1b, the geometry is described in terms of θ and φ , these two parameters are dependent on each other, where

$$\varphi = 2 \sin^{-1} \left(\frac{a_2}{c_3} \sin \left(\frac{\theta}{2} \right) \right). \quad (1)$$

Referring to Fig. 1b, the structure is oriented in space such that the two cuboids of dimensions $a_1 \times b_1 \times c_1$ have their edges of length b_1 aligned parallel to the Ox_2 direction while the edges of length a_1 and c_1 are aligned along the Ox_1 and Ox_3 directions, respectively. In this way, one of the remaining two sets of cuboids are then free to rotate in the Ox_1 – Ox_2 plane while the other set can rotate in the Ox_2 – Ox_3 plane.

Given this orientation, the projections, X_1, X_2 and X_3 along the Ox_1, Ox_2 and Ox_3 directions for this unit cell can be expressed in terms of the geometric parameters and the variable θ (or φ) by:

$$X_1 = a_1 + 2 \left(a_2 \cos \left(\frac{\theta}{2} \right) + b_2 \sin \left(\frac{\theta}{2} \right) \right), \quad (2)$$

$$X_2 = 2 \left(b_1 + a_2 \sin \left(\frac{\theta}{2} \right) \right) \equiv 2 \left(b_1 + c_3 \sin \left(\frac{\varphi}{2} \right) \right), \quad (3)$$

$$\begin{aligned} X_3 &= c_1 + 2 \left(c_3 \cos \left(\frac{\varphi}{2} \right) + b_3 \sin \left(\frac{\varphi}{2} \right) \right) \\ &\equiv c_1 + 2 \left(\sqrt{c_3^2 - a_2^2 \sin^2 \left(\frac{\theta}{2} \right)} + \frac{b_3 a_2}{c_3} \sin \left(\frac{\theta}{2} \right) \right). \end{aligned} \quad (4)$$

Since the units are assumed to be rigid, the changes dX_1, dX_2 and dX_3 along the Ox_1, Ox_2 and Ox_3 directions can be

¹ It should be noted that cuboids of this type from adjacent cells are connected together to form a single cuboid of length $2b_1$.

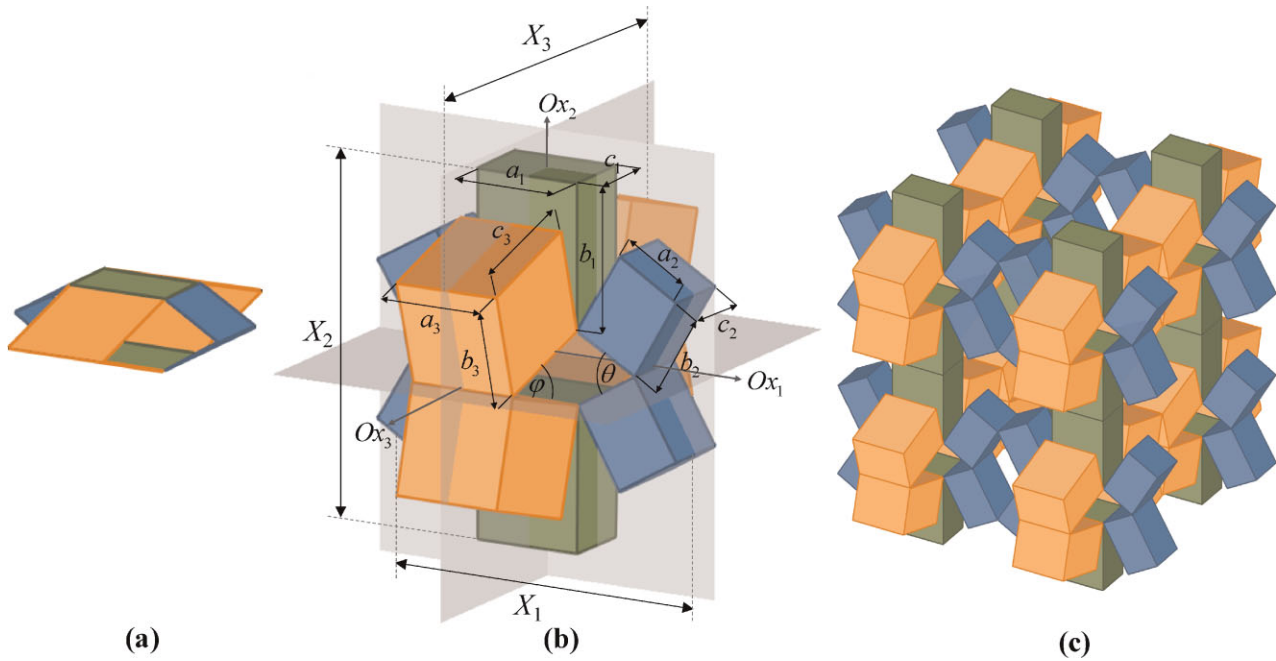


Figure 1 (online colour at: www.pss-b.com) (a) Two hexagonal honeycombs connected perpendicularly to each other, to which cuboids can be attached to generate the rotating cubes structure in (b). This structure is tessellatable and can be used to construct larger systems as shown in (c).

found by differentiating Eqs. (2)–(4) with respect to the single variable θ so that the resulting strains are given by:

$$\begin{aligned} \varepsilon_1 &= \frac{dX_1}{X_1} = \frac{1}{X_1} \left(\frac{dX_{11}}{d\theta} \right) d\theta \\ &= \frac{1}{X_1} \left(b_2 \cos\left(\frac{\theta}{2}\right) - a_2 \sin\left(\frac{\theta}{2}\right) \right) d\theta, \end{aligned} \quad (5)$$

$$\begin{aligned} \varepsilon_2 &= \frac{dX_2}{X_2} = \frac{1}{X_2} \left(\frac{dX_{22}}{d\theta} \right) d\theta \equiv \frac{1}{X_2} \left(\frac{dX_2}{d\varphi} \right) d\varphi \\ &= \frac{a_2}{X_2} \cos\left(\frac{\theta}{2}\right) d\theta \equiv \frac{c_3}{X_2} \cos\left(\frac{\varphi}{2}\right) d\varphi, \end{aligned} \quad (6)$$

$$\begin{aligned} \varepsilon_3 &= \frac{dX_3}{X_3} = \frac{1}{X_3} \left(\frac{dX_3}{d\varphi} \right) d\varphi = \frac{1}{X_3} \left(b_3 \cos\left(\frac{\varphi}{2}\right) - c_3 \sin\left(\frac{\varphi}{2}\right) \right) d\varphi \\ &\equiv \frac{1}{X_3} \frac{\left(b_3 \cos\left(\frac{\varphi}{2}\right) - c_3 \sin\left(\frac{\varphi}{2}\right) \right) a_2 \cos\left(\frac{\theta}{2}\right) d\theta}{c_3 \cos\left(\frac{\varphi}{2}\right)}. \end{aligned} \quad (7)$$

The corresponding Poisson's ratios are then given by:

$$\nu_{12} = (\nu_{21})^{-1} = -\frac{\varepsilon_2}{\varepsilon_1} = -\frac{X_1}{X_2} \frac{a_2 \cos\left(\frac{\theta}{2}\right)}{\left(b_2 \cos\left(\frac{\theta}{2}\right) - a_2 \sin\left(\frac{\theta}{2}\right) \right)}, \quad (8)$$

$$\begin{aligned} \nu_{13} &= (\nu_{31})^{-1} = -\frac{\varepsilon_3}{\varepsilon_1} \\ &= -\frac{X_1}{X_3} \frac{a_2 \cos\left(\frac{\theta}{2}\right) \left(b_3 \cos\left(\frac{\varphi}{2}\right) - c_3 \sin\left(\frac{\varphi}{2}\right) \right)}{c_3 \cos\left(\frac{\varphi}{2}\right) \left(b_2 \cos\left(\frac{\theta}{2}\right) - a_2 \sin\left(\frac{\theta}{2}\right) \right)}, \end{aligned} \quad (9)$$

$$\nu_{23} = (\nu_{32})^{-1} = -\frac{\varepsilon_3}{\varepsilon_2} = -\frac{X_2}{X_3} \frac{\left(b_3 \cos\left(\frac{\varphi}{2}\right) - c_3 \sin\left(\frac{\varphi}{2}\right) \right)}{c_3 \cos\left(\frac{\varphi}{2}\right)}. \quad (10)$$

2.2 The two-dimensional models An alternative approach to model the properties of 3D systems such as the one presented in the previous section is to consider only the 2D projection of a particular plane. Such an approach has been used, for example to explain the auxeticity of α -cristobalite in the (100) and (010) plane, a system constructed from 3D tetrahedra [23–25, 37], in terms of a 2D rotating rectangles model, where the rectangles are the 2D projection of the framework in these planes [26, 27].

In this case, it is interesting to note that it is possible for the 3D structure described in the previous section to have simpler 2D counterparts. For example, for some particular planes, the 2D model of the structure would be constructed from rectangles connected at their corners instead of cuboids connected at their edges. As shown in Fig. 2, a 2D

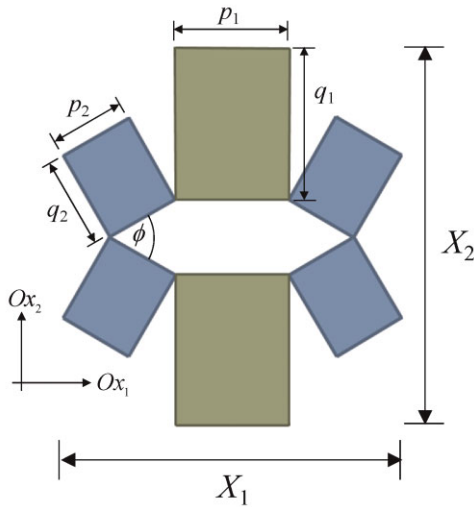


Figure 2 (online colour at: www.pss-b.com) A two-dimensional version of the 3-D model proposed in this paper.

representation of the system projected in the Ox_1-Ox_2 plane or the Ox_2-Ox_3 plane is one where the unit cell contains two $p_1 \times q_1$ rectangles and four $p_2 \times q_2$ rectangles. In this case, the system has two lines of symmetry which are parallel to the Ox_1 and Ox_2 directions. In such a symmetric system, five variables are required to define the geometry: p_1 , q_1 , p_2 , q_2 and ϕ . If it is assumed that the rectangles remain perfectly rigid during deformation then ϕ will be the only variable parameter. Note that this structure in fact corresponds to the projection of one of the faces of the 3D structure oriented parallel to Ox_1-Ox_2 plane or the Ox_2-Ox_3 plane.

If this planar structure is oriented in a similar way as its 3D version, i.e. the rectangles of dimensions $p_1 \times q_1$ are oriented such that q_1 is aligned parallel to the Ox_2 direction while p_1 is aligned parallel to the Ox_1 direction whilst the remaining rectangles are allowed to rotate in the Ox_1-Ox_2 plane, then the dimensions X_{11} and X_{22} along the Ox_1 and Ox_2 directions can be expressed as follows:

$$X_{11} = p_1 + 2 \left(p_2 \cos\left(\frac{\varphi}{2}\right) + q_2 \sin\left(\frac{\varphi}{2}\right) \right), \quad (11)$$

$$X_{22} = 2 \left(q_1 + p_2 \sin\left(\frac{\varphi}{2}\right) \right). \quad (12)$$

The strains which result from the deformation of the structure are then given by:

$$\varepsilon_1 = \frac{dX_{11}}{X_{11}} = \frac{1}{X_{11}} \left(q_2 \cos\left(\frac{\varphi}{2}\right) - p_2 \sin\left(\frac{\varphi}{2}\right) \right) d\varphi, \quad (13)$$

$$\varepsilon_2 = \frac{dX_{22}}{X_{22}} = \frac{p_2}{X_{22}} \cos\left(\frac{\varphi}{2}\right) d\varphi, \quad (14)$$

so that the Poisson's ratio in the Ox_1-Ox_2 plane can be given by:

$$\nu_{12}^* = (\nu_{21}^*)^{-1} = -\frac{\varepsilon_{22}}{\varepsilon_{11}} = -\frac{X_{11}}{X_{22}} \frac{p_2 \cos\left(\frac{\varphi}{2}\right)}{\left(q_2 \cos\left(\frac{\varphi}{2}\right) - p_2 \sin\left(\frac{\varphi}{2}\right) \right)}. \quad (15)$$

3 Results and discussion Typical plots for the six on-axis Poisson's ratios of the 3D model are shown in Figs. 3 and 4. In these plots, we consider a total of nine different cases which cover some of the possible configurations of the system ranging from the simplest one in (a) which is made up from identical cubes to a more generalised one in (i) made from cuboids of different size. More specifically cases (b) to (e) explore the effect of parameter b_i on the Poisson's ratio. These cases represent structures where the units correspond to cuboids having an identical square base (the side which forms part of the honeycomb cell shown in Fig. 1a). In (b) the cuboids are all identical, i.e. their height b_i is the same while in (c) and (d) one set of cuboids has a different height from the other two which are identical and in (e) each set of cuboids have a different height. Cases (f) to (h), on the other hand explore the effect of changing the dimensions of the faces of the honeycomb cell while the height of the cuboids b_i are equal and kept fixed. In case (f) the horizontal face, i.e. the base of the vertical cuboids is a square while that of the other two sets of inclined cuboids are rectangular and identical. In (g) all the cuboids are identical and with a rectangular base while in (h) each set of cuboids has different base dimensions.

From the graphs one can immediately note that in cases where the cuboids are not identical the range of values that θ can have may be limited. In fact, for geometries having b_2 or b_3 greater than b_1 , the minimum value that θ can have is limited by the conditions $b_2 \cos(\theta/2) \leq b_1$ for $b_2 > b_1$ or $b_3 \cos(\varphi/2) \leq b_1$ for $b_3 > b_1$. Similarly, there may also be an upper limit to the θ -value which occurs for instances where $a_2 > c_3$. For such geometries the maximum value that θ can have has to satisfy the condition that $\sin(\theta/2) \leq c_3/a_2$. These conditions establish a range of θ values which will ensure that the structure is physically realisable.

As illustrated in these plots, the equations derived here suggest that the Poisson's ratios for the proposed rotating rigid cuboids structure can be such that it may simultaneously exhibit negative values for all the six on-axis Poisson's ratios. In fact, it is evident from these plots, as well as from the equations, that there is always a plane for which the Poisson's ratio is negative and that it is possible to have systems which exhibit auxeticity in all three directions simultaneously. This is particularly true for the lower values of θ . This is very significant as it clearly shows the potential of such 3D models for achieving auxetic behaviour.

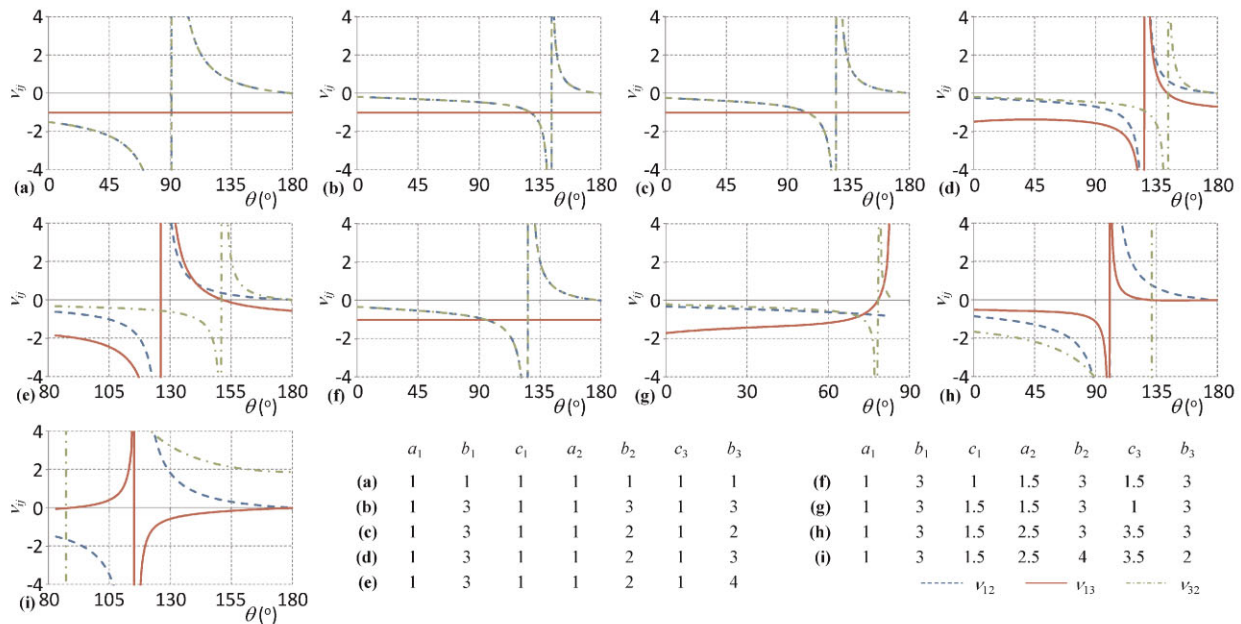


Figure 3 (online colour at: www.pss-b.com) Variation of the Poisson's ratios ν_{12} , ν_{13} and ν_{32} with the degree of openness (θ) for various rotating rigid cuboids systems showing that at low values of θ , all the systems considered exhibit auxeticity in all three directions simultaneously.

Before continuing any further, it is worth examining the manner in which such 3D systems may be constructed. In particular, it should be noted that on a 2D level, for the rotating rigid unit mechanism to be able to operate, the units must necessarily be connected at their corners. Contrary to

this, in systems consisting of 3D units, there is more than one way how they can be connected to each other – either at their corners, at their edges or even a combination of both. When the units are connected at their corners, their movement is much less constrained and can move in a similar way as if

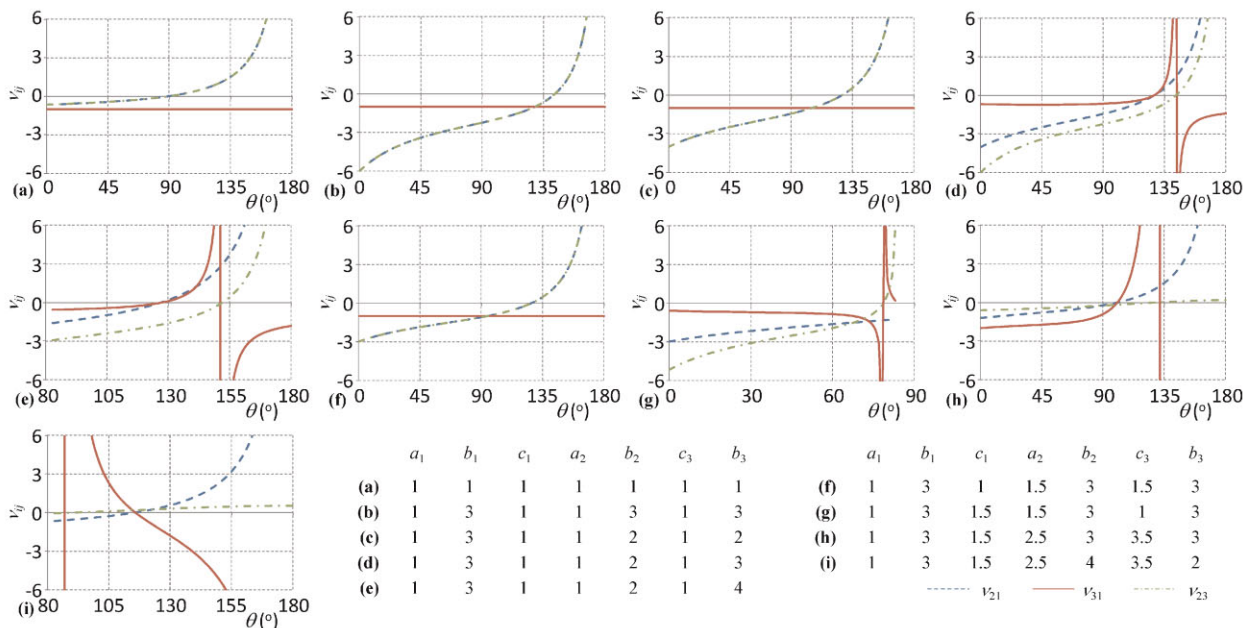


Figure 4 (online colour at: www.pss-b.com) Variation of the Poisson's ratios ν_{21} , ν_{31} and ν_{23} with the degree of openness (θ) for various rotating rigid cuboids systems showing that at low values of θ , all the systems considered exhibit auxeticity in all three directions simultaneously.

connected by a ball joint, which means that this connection may impart on the model two degrees of freedom which may be represented through the two Euler angles. On the other hand, when connected at their edges, the units are constrained to rotate in one plane only and thus only one degree of freedom may be associated with this mode of connection as is the case in the system presented here. In fact, such 'edge hinges' can be considered as being analogous to the hinges in 2D systems so that if one looks at the structure from a direction which is parallel to the hinging axis, then one would effectively observe a '2D system' made from units connected at their corners. Although, *prima facie* this may appear as offering no additional benefits to the 2D systems, it should be remembered that 3D polyhedral units have edges lying in different planes, thus facilitating the construction of 3D systems.

If one had to look at the equations for the mechanical properties of the 2D and 3D models derived, one will note the remarkable similarity in form between the expressions for the Poisson's ratios derived in the two approaches. In particular, the 2D expression for the Poisson's ratio ν_{12}^* has the same form as the equations for ν_{12} and ν_{32} in the 3D model and can be directly used to express these Poisson's ratios by replacing the 2D geometric parameters p_i , q_i and ϕ with the respective parameters a_i , b_i , c_i , θ and/or φ . Similar arguments can be made for the Poisson's ratios in these planes for loading in the Ox_2 direction. This is significant as it clearly shows the important role of the very simple 2D model to explain the properties of more complex 3D structures and gives added confidence to similar work based on this approach [26, 27, 38, 40, 60]. However, it should also be noted that it is not always possible to use this simple approach. For example, it should be noted that the Poisson's ratios in the Ox_1-Ox_3 plane, cannot be derived as easily in terms of a simple 2D model involving rotations. In this respect, if one had to use the 2D approach, an analysis of the deformations projected in the Ox_1-Ox_3 plane would have indicated a dilation type mechanism, something which would be analogous to the pioneering work by Wojciechowski and Branka [49] and Rothenburg et al. [48]. Obviously, this dilatary-like deformation is in reality a consequence of the rotational deformations which occur in the other two orthogonal planes: the negative Poisson's ratio in the Ox_1-Ox_3 plane is resulting due to the fact that the 3D topology of the system is such that the extent of dilation of the elements parallel to the Ox_1 direction (a 2D projection of units rotating in an orthogonal plane) are dependent on that of the elements parallel to the Ox_3 direction (also a 2D projection of units rotating in an orthogonal plane).

If one analyses the expressions presented above in more detail, one may note that the 2D models suggests that for ν_{12} , since $\cos(\varphi)$ is always positive, then a negative ν_{12} requires that the denominator in Eq. (15) is positive, i.e.

$$\nu_{12}^* : \frac{q_2}{p_2} > \tan\left(\frac{\varphi}{2}\right), \quad (16)$$

and obviously, since ν_{21}^* is the reciprocal of ν_{12}^* , the same conditions apply for a negative ν_{21}^* .

If this information is transposed to the 3D model, then this requirement becomes:

$$\nu_{12} : \frac{b_2}{a_2} > \tan\left(\frac{\theta}{2}\right), \quad (17)$$

and

$$\nu_{23} : \frac{b_3}{c_3} > \tan\left(\frac{\varphi}{2}\right), \quad (18)$$

or in terms of θ :

$$\nu_{23} : \frac{b_3}{c_3} > \sin\left(\frac{\theta}{2}\right) \left(\frac{c_3^2}{a_2^2} - \sin^2\left(\frac{\theta}{2}\right)\right)^{-1/2}. \quad (19)$$

Note that once again, the conditions for negative ν_{21} and ν_{32} are the same as those for negative ν_{12} and ν_{23} , respectively, since these are the reciprocal of each other. Thus, if both of these conditions are satisfied, then it is easy to show that for loading in the Ox_2 direction, the Poisson's ratio can be simultaneously negative in the Ox_1-Ox_2 plane and Ox_2-Ox_3 plane. Also, in the case of the Poisson's ratio in the Ox_1-Ox_3 plane, in the absence of the simple 2D model equivalent, one must look directly at the 3D model. Here, one notes that for negative ν_{13} , the requirements are similar to those above, and for it to be negative, there are two conditions which need to be satisfied simultaneously:

$$\nu_{13} : \begin{cases} \frac{b_2}{a_2} > \tan\left(\frac{\theta}{2}\right) \text{ and } \frac{b_3}{c_3} > \sin\left(\frac{\theta}{2}\right) \left(\frac{c_3^2}{a_2^2} - \sin^2\left(\frac{\theta}{2}\right)\right)^{-1/2} \\ \text{or} \\ \frac{b_2}{a_2} < \tan\left(\frac{\theta}{2}\right) \text{ and } \frac{b_3}{c_3} < \sin\left(\frac{\theta}{2}\right) \left(\frac{c_3^2}{a_2^2} - \sin^2\left(\frac{\theta}{2}\right)\right)^{-1/2} \end{cases}. \quad (20)$$

Thus, it can be shown from the equations that given that both of the conditions $\tan(\theta/2) < b_2/a_2$ and $\tan(\varphi/2) < b_3/c_3$ are satisfied, then all the on-axis Poisson's ratios are negative.

At this point, it is important to understand what happens when the structure deforms in order to understand when it can exhibit auxetic behaviour. When a tensile force is applied along the Ox_2 direction, the structure responds by increasing θ and φ and the inclined cuboids rotate accordingly away from the vertical cuboids to occupy more space. The largest possible dimensions of the unit cell in the Ox_1 direction is determined by the diagonal of the inclined cuboids lying in the Ox_1-Ox_2 plane and correspond to a configuration where the diagonal of the inclined cuboids lies horizontally, i.e. when $\tan(\theta/2) = b_2/a_2$. Referring to Eq. (8), these conditions in fact correspond to a continuous transition of the Poisson's ratio ν_{21} in the Ox_1-Ox_2 plane from a negative to a positive value. Thus, until the

structure reaches this point, it is auxetic in the relevant plane. However, if θ allows, stretching any further will cause the diagonal to go past this point so the respective unit cell dimension decreases and the structure starts to behave conventionally in this plane. Beyond this point the Poisson's ratio becomes increasingly positive, towards a value of:

$$\nu_{21} = -\frac{X_2}{X_1} \left[\frac{b_2}{a_2} - \frac{c_3}{\sqrt{a_2^2 - c_3^2}} \right],$$

when $a_2 > c_3$ and to very high values when $c_3 \geq a_2$ as θ tends to its maximum value. The Ox_2 – Ox_3 plane behaves in a similar way where the Poisson's ratios tend to very high values when $a_2 \geq c_3$ and to:

$$\nu_{23} = -\frac{X_2}{X_1} \left[\frac{b_3}{c_3} - \frac{a_2}{\sqrt{c_3^2 - a_2^2}} \right],$$

when $c_3 > a_2$ as θ tends to its maximum value.

Similarly, on stretching in the Ox_1 direction, θ also increases and the Ox_1 – Ox_2 plane is also auxetic. However, when the structure reaches the conformation where the diagonal of the cuboids in this plane becomes aligned with the horizontal, then the structure becomes locked in that configuration and can be stretched no further. However, this barrier can be overcome by applying a moment to the cuboids to force them past this barrier after which the structure shows conventional behaviour in this plane. In fact, this change in sign of the Poisson's ratio is characterised by an asymptotic transition at the point where $b_2/a_2 = \tan(\theta/2)$. Following this transition, the Poisson's ratio becomes highly positive and starts to decrease to a lower value of:

$$\nu_{12} = -\frac{X_1}{X_2} \left[\frac{b_2}{a_2} - \frac{c_3}{\sqrt{a_2^2 - c_3^2}} \right]^{-1},$$

if $a_2 > c_3$ or 0 if $c_3 > a_2$, as θ reaches its maximum value. A similar analysis also applies for loading in the Ox_3 direction.

In the case of the Ox_1 – Ox_3 plane, the Poisson's ratio ν_{13} can be expressed in terms of the Poisson's ratio for the other two planes as follows:

$$\nu_{13} = (\nu_{31})^{-1} = -\frac{\nu_{12}}{\nu_{32}}.$$

This relation suggests that when ν_{12} tends to 0 or ν_{32} approaches very high magnitudes, ν_{13} tends to 0. Similarly, ν_{13} tends to high magnitudes of Poisson's ratio when ν_{32} approaches 0 or when ν_{12} tends towards large magnitudes.

Before concluding, it should be noted that 3D systems may not only be constructed from polyhedra, but other shapes can be used including 2D plates (example polygons), and 1D fibres or rod-like units. For example, the system in Fig. 5 modelled by Grima [52] and Gaspar et al. [61] represents an example of one such 3D system made from cuboids and fibrils, which system achieves auxeticity through the re-entrant mechanism. Nevertheless, as explained by Grima [52], this system could easily be converted to one which would have involved rotation of

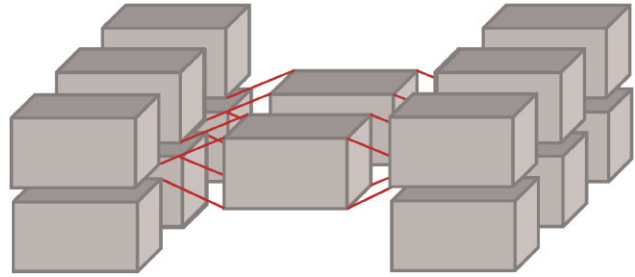


Figure 5 (online colour at: www.pss-b.com) The 3D system proposed and modelled by Grima [52] and Gaspar et al. [61].

the cuboidal units, for example through the 'chiral mechanism'.

In view of all this, it is obvious that the 3D system proposed and modelled here is only one of the many structures which may be constructed from connected cuboids. It is not within the scope of this work to fully investigate and characterise such systems but Fig. 6 illustrates one other system which can be constructed from cuboids, where the cuboids are connected at their corners rather than from their edges. Preliminary investigations using finite element methods on such a system where the cuboids are 'fused' together suggest that it can also exhibit negative Poisson's ratios.

Also, in this derivation, a highly idealised scenario was considered since it was assumed that the cuboidal units (or their 2D rectangular projection) remain perfectly rigid, something which in real scenarios is difficult to achieve. In this respect it should be highlighted that the expressions for the Poisson's ratio derived here are scale independent, i.e.

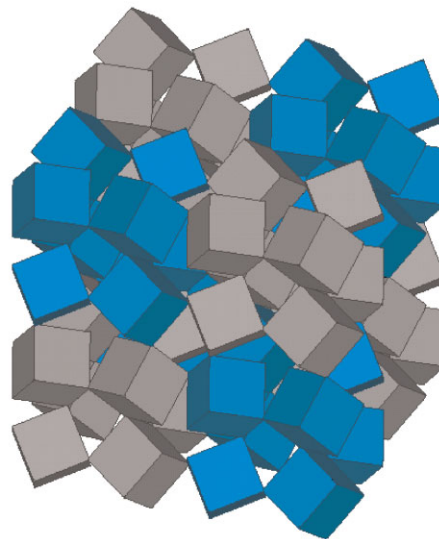


Figure 6 (online colour at: www.pss-b.com) A 3D system that can be constructed from cuboids that are connected from their corners and which has a potential to exhibit auxetic behaviour. Different colours are used to distinguish adjacent unit cells.

they can be used to downscale the design to the micro- or nanoscale so as to achieve a system which can be considered as an auxetic material rather than an auxetic structure. Furthermore, the models derived here may find use to explain the auxeticity in already existent (man-made or naturally occurring) auxetics. Obviously, in such systems, it is even more unrealistic to assume that behaviour is as idealistic as the one described here, and it is clear that the model presented here would need to be extended to include additional modes of deformation.

4 Conclusions In this work, it has been shown that the concept of using rotating rigid units for achieving auxetic behaviour in 2D may easily be transposed to 3D hence obtaining auxetic systems which may exhibit auxeticity in more than one plane. In fact, a simple system constructed from rigid cuboidal units connected together at their edges was proposed and it was shown through detailed analytical modelling that it may exhibit simultaneously negative Poisson's ratios in its three major planes.

It was also shown that in such systems, there may still be an important role for the simpler 2D modelling approach which considers only particular projections of the more complex 3D systems, although in some cases (or projections) this may be more difficult to accomplish.

In view of the high extent of auxeticity of this system, particularly its ability to exhibit simultaneously negative Poisson's ratio ν_{ij} ($i, j = 1, 2, 3$), it is hoped that this work will stimulate additional work which will attempt to design and construct real auxetics at any scale (the Poisson's ratio is a scale independent property) which are based on the models presented here.

References

- [1] K. E. Evans, M. A. Nkansah, I. J. Hutchinson, and S. C. Rogers, *Nature* **253**, 124 (1991).
- [2] R. S. Lakes, *Science* **235**, 1038–1040 (1987).
- [3] N. Chan and K. E. Evans, *J. Cellular Plast.* **34**, 231–260 (1998).
- [4] K. L. Alderson, A. P. Pickles, P. J. Neale, and K. E. Evans, *Acta Metall. Mater.* **42**, 2261–2266 (1994).
- [5] K. L. Alderson, A. Fitzgerald, and K. E. Evans, *J. Mater. Sci.* **35**, 4039–4047 (2000).
- [6] C. W. Smith, F. Lehman, R. J. Wootton, and K. E. Evans, *Cell. Polym.* **18**, 79–101 (1999).
- [7] A. Alderson, J. Rasburn, S. Ameer-Beg, P. G. Mullarkey, W. Perrie, and K. E. Evans, *Ind. Eng. Chem. Res.* **39**, 654–665 (2000).
- [8] A. Alderson, J. Rasburn, K. E. Evans, and J. N. Grima, *Membr. Technol.* **137**, 6–8 (2001).
- [9] J. Rasburn, P. G. Mullarkey, K. E. Evans, A. Alderson, S. Ameer-Beg, and W. Perrie, *AiChE J.* **47**, 2623–2626 (2001).
- [10] C. P. Chen and R. S. Lakes, *Cell. Polym.* **8**, 343–369 (1989).
- [11] C. P. Chen and R. S. Lakes, *J. Eng. Mater. Technol. (ASME)* **118**, 285–288 (1996).
- [12] B. Howell, P. Prendergast, and L. Hansen, *Acoustic Behaviour of Negative Poisson's Ratio Materials* (David Taylor Research Center, Bethesda Md, Ship Materials Engineering Dept., 1991).
- [13] F. Scarpa and G. Tomlinson, *J. Sound Vib.* **230**, 45–67 (2000).
- [14] F. Scarpa, L. G. Ciffo, and Y. R. Yates, *Smart Mater. Struct.* **13**, 49–56 (2004).
- [15] F. Scarpa, W. A. Bullough, and P. Lumley, *Proc. Inst. Mech. Eng. C: J. Mech. Eng. Sci.* **218**, 241–244 (2004).
- [16] L. J. Gibson, M. F. Ashby, G. S. Schajer, and C. I. Robertson, *Proc. R. Soc. Lond. A* **382**, 25–42 (1982).
- [17] I. G. Masters and K. E. Evans, *Compos. Struct.* **35**, 403–422 (1996).
- [18] F. Scarpa, *Compos. Sci. Technol.* **70**, 1033 (2010).
- [19] A. Yeganeh-Haeri, D. J. Weidner, and J. B. Parise, *Science* **257**, 650–652 (1992).
- [20] N. R. Keskar and J. R. Chelikowsky, *Nature* **358**, 222–224 (1992).
- [21] N. R. Keskar and J. R. Chelikowsky, *Phys. Rev. B* **48**, 227–233 (1993).
- [22] H. Kimizuka, H. Kaburaki, and Y. Kogure, *Phys. Rev. Lett.* **84**, 5548–5551 (2000).
- [23] A. Alderson and K. E. Evans, *Phys. Chem. Miner.* **28**, 711–718 (2001).
- [24] A. Alderson and K. E. Evans, *Phys. Rev. Lett.* **89**, 225503 (2002).
- [25] A. Alderson and K. E. Evans, *J. Phys.: Condens. Matter* **21**, 025401 (2009).
- [26] J. N. Grima, R. Gatt, A. Alderson, and K. E. Evans, *J. Mater. Chem.* **15**, 4003–4005 (2005).
- [27] J. N. Grima, A. Alderson, and K. E. Evans, *Mater. Sci. Eng. A* **423**, 219–224 (2006).
- [28] J. N. Grima, R. Jackson, A. Alderson, and K. E. Evans, *Adv. Mater.* **12**, 1912–1928 (2000).
- [29] J. N. Grima, R. Gatt, V. Zammit, J. J. Williams, A. Alderson, and R. I. Walton, *J. Appl. Phys.* **101**, 86102 (2007).
- [30] J. N. Grima, P. S. Farrugia, C. Caruana, R. Gatt, and D. Attard, *J. Mater. Sci.* **43**, 5962–5971 (2008).
- [31] J. J. Williams, C. W. Smith, K. E. Evans, Z. A. D. Lethbridge, and R. I. Walton, *Acta Mater.* **55**, 5697–5707 (2007).
- [32] K. E. Evans, M. A. Nkansah, and I. J. Hutchinson, *Acta Metall. Mater.* **42**, 1289–1294 (1994).
- [33] K. E. Evans, A. Alderson, and F. R. Christian, *J. Chem. Soc. Faraday Trans.* **91**, 2671–2680 (1995).
- [34] J. B. Choi and R. S. Lakes, *Int. J. Mech. Sci.* **37**, 51–59 (1995).
- [35] A. Bezazi, F. Scarpa, and C. Remillat, *Compos. Struct.* **71**, 356–364 (2005).
- [36] O. Sigmund, *Mech. Mater.* **20**, 351–368 (1995).
- [37] A. Alderson, K. L. Alderson, K. E. Evans, J. N. Grima, M. R. Williams, and P. J. Davies, *Comput. Methods Sci. Technol.* **10**, 117–126 (2004).
- [38] J. N. Grima and K. E. Evans, *J. Mater. Sci. Lett.* **19**, 1563–1565 (2000).
- [39] J. N. Grima, A. Alderson, and K. E. Evans, *Phys. Status Solidi B* **242**, 561–575 (2005).
- [40] J. N. Grima, V. Zammit, R. Gatt, A. Alderson, and K. E. Evans, *Phys. Status Solidi B* **224**, 866–882 (2007).
- [41] K. W. Wojciechowski, *Phys. Lett. A* **137**, 60–64 (1989).
- [42] M. Kowalik and K. W. Wojciechowski, *Phys. Status Solidi B* **242**, 626–631 (2005).
- [43] K. V. Tretiakov and K. W. Wojciechowski, *Phys. Status Solidi B* **244**, 1038–1046 (2007).

- [44] K. W. Wojciechowski, *J. Phys. A* **36**, 11765–11778 (2003).
- [45] K. W. Wojciechowski, K. V. Tretiakov, and M. Kowalik, *Phys. Rev. E* **67**, 036121 (2003).
- [46] J. W. Narojczyk and K. W. Wojciechowski, *Phys. Status Solidi B* **245**, 2463–2468 (2008).
- [47] V. V. Novikov and K. W. Wojciechowski, *Phys. Solid State* **41**, 1970–1975 (1999).
- [48] L. Rothenburg, A. A. Berlin, and R. J. Bathurst, *Nature* **354**, 470–472 (1991).
- [49] K. W. Wojciechowski and A. C. Branka, *Mol. Phys. Rep.* **6**, 71 (1994).
- [50] R. Lakes and K. W. Wojciechowski, *Phys. Status Solidi B* **245**, 545–551 (2008).
- [51] K. E. Evans and A. Alderson, *Adv. Mater.* **12**, 617–628 (2000).
- [52] J. N. Grima, *New Auxetic Materials*, Ph.D. dissertation, University of Exeter (2000).
- [53] A. Alderson, *Chem. Ind.* 384–391 (1999).
- [54] P. V. Pikhitsa, *Phys. Rev. Lett.* **93**, 15505 (2004).
- [55] D. Prall and R. S. Lakes, *Int. J. Mech. Sci.* **39**, 305–314 (1997).
- [56] J. N. Grima, R. Gatt, and P. S. Farrugia, *Phys. Status Solidi B* **245**, 511–520 (2008).
- [57] J. N. Grima, A. Alderson, and K. E. Evans, *J. Phys. Soc. Jpn.* **74**, 1341–1342 (2005).
- [58] S. A. McDonald, N. Ravirala, P. J. Withers, and A. Alderson, *Scr. Mater.* **60**, 232–235 (2009).
- [59] J. N. Grima, V. Zammit, R. Gatt, D. Attard, C. Caruana, and T. G. Chircop Bray, *J. Non-Cryst. Solids* **354**, 4214–4220 (2008).
- [60] J. J. Williams, C. W. Smith, K. E. Evans, Z. A. D. Lethbridge, and R. I. Walton, *Chem. Mater.* **19**, 2423–2434 (2007).
- [61] N. Gaspar, C. W. Smith, A. Alderson, J. N. Grima, and K. E. Evans, *J. Mater. Sci.* **46**, 372–384 (2011).